POLITECNICO DI TORINO
Repository ISTITUZIONALE

Improved Harmonic Balance implementation of Floquet analysis for nonlinear circuit simulation

Original
Improved Harmonic Balance implementation of Floquet analysis for nonlinear circuit simulation / Traversa F.L.; Bonani F.. - In: AEÜ. INTERNATIONAL JOURNAL OF ELECTRONICS AND COMMUNICATIONS. - ISSN 1434-8411. - STAMPA. - 66:5(2012), pp. 357-363. [10.1016/j.aeue.2011.09.002]

Availability:
This version is available at: 11583/2455375 since:

Publisher:
Elsevier

Published
DOI:10.1016/j.aeue.2011.09.002

Terms of use:
openAccess

This article is made available under terms and conditions as specified in the corresponding bibliographic description in the repository

Publisher copyright

(Article begins on next page)

06 December 2021

AEÜ Int. J. Electron. Commun.
51 (1997) No. 1, 1–1
© Gustav Fischer Verlag
Jena

Improved Harmonic Balance Implementation of Floquet Analysis for Nonlinear Circuit Simulation

Fabio L. Traversa, Fabrizio Bonani

Abstract **We present a novel algorithm for the efficient numerical computation of the Floquet quantities (eigenvalues, direct and adjoint eigenvectors) relevant to the assessment of the stability and noise properties of nonlinear forced and autonomous circuits. The approach is entirely developed in the frequency domain by means of the application of the Harmonic Balance technique, thus avoiding lengthy time-frequency transformations which might also impair the accuracy of the calculated quantities. An improvement in the computation time around one order of magnitude is observed.**

Keywords **Circuit simulation, Floquet theory, Frequency domain analysis, Harmonic Balance.**

Floquet analysis, although a classical topic in the mathematical literature [1, 2], is the object of a renewed interest in the circuit simulation community because of the central role played in two important areas of nonlinear circuit performance assessment: the rigorous study of phase and amplitude noise in oscillators [3, 4, 5, 6, 7, 8], and the appraisal of the stability of the time-periodic working point solution of a nonlinear circuit, either driven or autonomous [1, 2, 9, 10, 11, 12, 13].

Floquet theorem was originally derived with reference to Ordinary Differential Equations (ODEs) [1], and recently has been extended to the case of index-1 Differential Algebraic Equations (DAEs) [14]. This step has significant practical importance, since DAE is the general form of the describing equations obtained from the application of nodal analysis to a nonlinear circuit made of lumped components [15]. In general, the circuit nodal equations can be cast in the form

$$\begin{bmatrix} \boldsymbol{L}_1 \dfrac{\mathrm{d}\boldsymbol{x}}{\mathrm{d}t} \\ \dfrac{\mathrm{d}}{\mathrm{d}t}\boldsymbol{f}(\boldsymbol{x}(t)) \end{bmatrix} = \begin{bmatrix} \boldsymbol{L}_2\boldsymbol{x} \\ \boldsymbol{g}(\boldsymbol{x}(t),t) \end{bmatrix} + \begin{bmatrix} \boldsymbol{c}(t) \\ \boldsymbol{d}(t) \end{bmatrix} \qquad (1)$$

where $\boldsymbol{x}(t) \in \mathbb{R}^n$ is the unknown vector, $\boldsymbol{L}_1, \boldsymbol{L}_2 \in \mathbb{R}^{m\times n}$ with $m \leq n$ are constant matrices describing the linear part of the circuit, $\boldsymbol{c}(t) \in \mathbb{R}^m$ and $\boldsymbol{f}, \boldsymbol{g}, \boldsymbol{d} \in \mathbb{R}^{n-m}$. The nonlinear functions $\boldsymbol{f}, \boldsymbol{g}$ are due to the nonlinear elements in the circuit. The forcing terms in (1) (if any) are time-periodic functions of period T, and a non-trivial T-periodic solution (limit cycle) $\boldsymbol{x}_\mathrm{S}(t)$ is assumed to exist[1].

Floquet theorem [14] applies to the linearization of (1) around $\boldsymbol{x}_\mathrm{S}(t)$, i.e. it is a tool to characterize the effect of a small-change perturbation applied to the circuit limit cycle (see [11] and references therein). The main result is that the stability of $\boldsymbol{x}_\mathrm{S}(t)$ is dependent on a set of n (complex) numbers λ_k $(k = 1, \ldots, n)$ called the *Floquet multipliers* (FMs) of $\boldsymbol{x}_\mathrm{S}(t)$: if all of them (or, for oscillators, all but one which is exactly equal to 1) are placed strictly inside the unit circle of the complex plane, the limit cycle is asymptotically stable; on the other hand, if at least one of them has magnitude larger than one, the solution is unstable. The computation of the FMs provides therefore an assessment of the stability of the circuit working point. On the other hand, each FM is also associated to a *(direct) Floquet eigenvector* $\boldsymbol{u}_k(t)$ $(k = 1, \ldots, n)$ which, together with the *adjoint Floquet eigenvectors* $\boldsymbol{v}_k(t)$ $(k = 1, \ldots, n)$ associated to the adjoint linearized system[2], are the basic ingredients required to perform oscillator noise analysis [3, 7, 8].

The calculation of the Floquet multipliers and eigenvectors can be performed either in the time or in the frequency domain. The problem has been traditionally tackled for ODEs in the time domain [16, 9, 17, 11], devising numerical approaches with various degrees of efficiency and accuracy. On the other hand for many applications spectral techniques, such as the harmonic balance (HB) method, provide significant advantages for the determination of the circuit limit cycle [15, 18, 19]. A general purpose, frequency-domain algorithm based on the HB approach for the determination of the direct and adjoint Floquet quantities was proposed in [10] and [20], respectively. In both cases, a generalized eigenvalue problem has to be solved, thus requiring a numerical procedure whose computational burden is $O(N^3)$ where N is the matrices size. Notice that for HB, $N = n(2N_\mathrm{H} + 1)$ where N_H is the number of harmonics included in the simulation besides DC. In this contribution, we propose a numerical approach applicable to both the direct and adjoint problem which, making use of fast matrix manipulation completely taking place in the frequency domain, allows for a significant advantage with respect to previous algorithms by reducing the computational complexity to $O(N^2)$. The algorithm ultimately corresponds to a general methodology for constructing a linear ODE fully equivalent to the linearized DAE, thus extending the applicability of the approach in [9, 16, 17].

1. Fundamentals

We provide here the fundamentals required to effectively present the numerical procedure we developed. Linearization of (1) around the limit cycle $\boldsymbol{x}_\mathrm{S}(t)$ leads to a Linear

[1] The same hypothesis holds for the case of autonomous circuits, for which of course no source term is present.

[2] Both the direct and adjoint linearized systems share the same FMs [1, 14].

Received month 00, 1997.

Dr. F.L. Traversa, Departament d'Enginyeria Electrònica, Universitat Autònoma de Barcelona, Bellaterra, 08193, Spain.
Prof. F. Bonani, Dipartimento di Elettronica, Politecnico di Torino, Corso Duca degli Abruzzi 24, Torino, 10129, Italy.

AEÜ Int. J. Electron. Commun.
51 (1997) No. 1, 1–1

Periodic Time Varying (LPTV) system of the form

$$\frac{\mathrm{d}}{\mathrm{d}t}[\boldsymbol{C}(t)\boldsymbol{z}] = \boldsymbol{A}(t)\boldsymbol{z}(t) \tag{2}$$

where $\boldsymbol{C}, \boldsymbol{A} \in \mathbb{R}^{n\times n}$ are T-periodic matrices (since they correspond to the jacobian of the full system calculated into $\boldsymbol{x}_{\mathrm{S}}(t)$) and $\boldsymbol{z}(t) \in \mathbb{R}^n$ represents the perturbation of the limit cycle. In many cases, matrix $\boldsymbol{C}(t)$ is not full rank although we assume that the rank $\rho \leq n$ is independent of time (index-1 DAE) [14]: this has important consequences on the calculation of the Floquet quantities, as we will see shortly.

According to the generalization of Floquet theorem to DAEs [14], (2) is solved by ρ independent functions taking the form $\boldsymbol{z}(t) = \exp(\mu_k t)\boldsymbol{u}_k(t)$ $(k = 1, \ldots, \rho)$, where $\mu_1, \ldots, \mu_\rho$ are the *Floquet exponents* (FEs) of (2) (and $\lambda_k = \exp(\mu_k T)$ are the corresponding *Floquet multipliers*), $\boldsymbol{u}_k(t)$ is T-periodic and is called the *direct Floquet eigenvector* associated to μ_k. Notice that $\rho < n$ corresponds to the appearance of $n - \rho$ FEs equal to $-\infty$.

On the other hand, the *adjoint* system to (2) reads [14]

$$\boldsymbol{C}^{\mathrm{T}}(t)\frac{\mathrm{d}\boldsymbol{w}}{\mathrm{d}t} = -\boldsymbol{A}^{\mathrm{T}}(t)\boldsymbol{w}(t) \tag{3}$$

and is solved by a linear combination of the ρ independent functions $\boldsymbol{w}(t) = \exp(-\mu_k t)\boldsymbol{v}_k(t)$, where $\boldsymbol{v}_k(t)$ is again T-periodic and is called the *adjoint Floquet eigenvector* associated to μ_k.

1.1 The HB technique

The HB technique is based on representing each scalar time periodic function $\alpha(t)$ through the (truncated) Fourier series

$$\alpha(t) = \tilde{\alpha}_{0,\mathrm{c}} + \sum_{h=1}^{N_{\mathrm{H}}} [\tilde{\alpha}_{h,\mathrm{c}}\cos(h\omega_0 t) + \tilde{\alpha}_{h,\mathrm{s}}\sin(h\omega_0 t)] \tag{4}$$

where $\tilde{\alpha}_{0,\mathrm{c}}$ represents the DC component of $\alpha(t)$. The harmonic components are collected into a vector of size $2N_{\mathrm{H}}+1$ $\tilde{\boldsymbol{\alpha}} = [\tilde{\alpha}_{0,\mathrm{c}}, \tilde{\alpha}_{1,\mathrm{c}}, \tilde{\alpha}_{1,\mathrm{s}}, \ldots, \tilde{\alpha}_{N_{\mathrm{H}},\mathrm{c}}, \tilde{\alpha}_{N_{\mathrm{H}},\mathrm{s}}]^{\mathrm{T}}$, and put in one-to-one correspondence with a set of $2N_{\mathrm{H}} + 1$ time samples (distributed into the interval $]0, T]$) of $\alpha(t)$, collected into vector $\hat{\boldsymbol{\alpha}} = [\alpha(t_1), \alpha(t_2), \ldots, \alpha(t_{2N_{\mathrm{H}}+1})]^{\mathrm{T}}$. The relationship between $\hat{\boldsymbol{\alpha}}$ and $\tilde{\boldsymbol{\alpha}}$ is provided by an invertible linear operator $\boldsymbol{\Gamma}^{-1}$ corresponding to the discrete Fourier transform (DFT) [15]

$$\hat{\boldsymbol{\alpha}} = \boldsymbol{\Gamma}^{-1}\tilde{\boldsymbol{\alpha}} \Longleftrightarrow \tilde{\boldsymbol{\alpha}} = \boldsymbol{\Gamma}\hat{\boldsymbol{\alpha}}. \tag{5}$$

Notice that the matrix representation is used for formal derivation only: in the actual implementation the more efficient DFT algorithm [15] is used.

Denoting as $\dot{\alpha}(t)$ the first derivative of $\alpha(t)$, trivial calculations yield the Fourier representation of the derivative as a function of the Fourier components of the original function

$$\tilde{\dot{\boldsymbol{\alpha}}} = \boldsymbol{\Gamma}\hat{\dot{\boldsymbol{\alpha}}} = \boldsymbol{\Omega}\tilde{\boldsymbol{\alpha}}, \tag{6}$$

where $\boldsymbol{\Omega} \in \mathbb{R}^{(2N_{\mathrm{H}}+1)\times(2N_{\mathrm{H}}+1)}$ is a tridiagonal costant matrix proportional to ω_0 (see [15, 10] for the explicit representation).

In case of an n size vector $\boldsymbol{\alpha}(t)$, (5) and (6) are easily generalized by considering a vector of time-sample vectors and frequency components, defined by expanding each element $\alpha_j(t)$ $(j = 1, \ldots, n)$ into the time sample $\hat{\boldsymbol{\alpha}}_j$ and similarly for the harmonic components. One finds

$$\hat{\boldsymbol{\alpha}} = \boldsymbol{\Gamma}_n^{-1}\tilde{\boldsymbol{\alpha}} \qquad \tilde{\dot{\boldsymbol{\alpha}}} = \boldsymbol{\Omega}_n\tilde{\boldsymbol{\alpha}}, \tag{7}$$

where $\boldsymbol{\Gamma}_n^{-1}$ and $\boldsymbol{\Omega}_n$ are block diagonal matrices built replicating n times the fundamental operators $\boldsymbol{\Gamma}^{-1}$ and $\boldsymbol{\Omega}$, respectively.

More attention is required to derive the HB representation of $\boldsymbol{\beta}(t) = \boldsymbol{\Xi}(t)\boldsymbol{\alpha}(t)$ and of its time derivative, where $\boldsymbol{\Xi}(t)$ is a T-periodic matrix and $\boldsymbol{\alpha}(t)$ a T-periodic vector. Denoting as $\hat{\boldsymbol{\Xi}}$ the $n \times n$ block diagonal matrix built expanding each element $\xi_{h,k}(t)$ of $\boldsymbol{\Xi}(t)$ as a $(2N_{\mathrm{H}} + 1) \times (2N_{\mathrm{H}} + 1)$ diagonal matrix formed by the time samples $\hat{\xi}_{h,k}$, we have

$$\tilde{\boldsymbol{\beta}} = \tilde{\boldsymbol{\Xi}}\tilde{\boldsymbol{\alpha}} \qquad \tilde{\dot{\boldsymbol{\beta}}} = \boldsymbol{\Omega}_n\tilde{\boldsymbol{\beta}} = \boldsymbol{\Omega}_n\tilde{\boldsymbol{\Xi}}\tilde{\boldsymbol{\alpha}} \tag{8}$$

where $\tilde{\boldsymbol{\Xi}} = \boldsymbol{\Gamma}_n\hat{\boldsymbol{\Xi}}\boldsymbol{\Gamma}_n^{-1}$. The transformation leading to $\tilde{\boldsymbol{\Xi}}$ results into the sum of a Toepliz and of a Hankel matrix (see [21] for details), whose building blocks are the Fourier coefficients of the elements of $\boldsymbol{\Xi}(t)$: in other words, $\tilde{\boldsymbol{\Xi}}$ can be easily assembled after evaluating (through DFT) the Fourier coefficients of the elements of $\boldsymbol{\Xi}(t)$.

2. Previous work

Substituting $\boldsymbol{z}(t) = \exp(\mu_k t)\boldsymbol{u}_k(t)$ into (2) and $\boldsymbol{w}(t) = \exp(-\mu_k t)\boldsymbol{v}_k(t)$ into (3), the Floquet direct and adjoint eigenproblems are made explicit in the time domain [10, 20]

$$\mu_k\boldsymbol{C}(t)\boldsymbol{u}_k(t) = \boldsymbol{A}(t)\boldsymbol{u}_k(t) - \frac{\mathrm{d}}{\mathrm{d}t}[\boldsymbol{C}(t)\boldsymbol{u}_k(t)] \tag{9}$$

$$\mu_k\boldsymbol{C}^{\mathrm{T}}(t)\boldsymbol{v}_k(t) = \boldsymbol{A}^{\mathrm{T}}(t)\boldsymbol{v}_k(t) + \boldsymbol{C}^{\mathrm{T}}(t)\frac{\mathrm{d}\boldsymbol{v}_k(t)}{\mathrm{d}t}. \tag{10}$$

After time-sampling, the use of (6) and (8) allows to convert (9) and (10) in the spectral domain

$$\mu_k\tilde{\boldsymbol{C}}\tilde{\boldsymbol{u}}_k = \left[\tilde{\boldsymbol{A}} - \boldsymbol{\Omega}_n\tilde{\boldsymbol{C}}\right]\tilde{\boldsymbol{u}}_k \tag{11}$$

$$\mu_k\tilde{\boldsymbol{C}}_{\mathrm{T}}\tilde{\boldsymbol{v}}_k = \left[\tilde{\boldsymbol{A}}_{\mathrm{T}} + \tilde{\boldsymbol{C}}_{\mathrm{T}}\boldsymbol{\Omega}_n\right]\tilde{\boldsymbol{v}}_k. \tag{12}$$

Notice that $\tilde{\boldsymbol{C}}_{\mathrm{T}} = \boldsymbol{\Gamma}_n\hat{\boldsymbol{C}}^{\mathrm{T}}\boldsymbol{\Gamma}_n^{-1}$ is not simply the transpose of $\tilde{\boldsymbol{C}}$ (the same holds for $\tilde{\boldsymbol{A}}_{\mathrm{T}}$). Nevertheless, since $\hat{\boldsymbol{C}}$ is made of diagonal blocks (deriving from the time-sampling of the elements of $\boldsymbol{C}(t)$), $\tilde{\boldsymbol{C}}_{\mathrm{T}}$ can easily be built from the components of $\tilde{\boldsymbol{C}}$ avoiding any further calculation [20]. In summary, the Floquet quantities can be calculated as the solution of the generalized eigenvalue problems in (11) and (12), whose matrices correspond to the jacobians of the HB problem defining the limit cycle, and therefore are available as a byproduct of the Newton iterations normally exploited for the determination of $\boldsymbol{x}_{\mathrm{S}}(t)$.

The solution of the generalized eigenproblems (11) and (12) yields $n(2N_{\mathrm{H}}+1)$ FEs (and the corresponding direct and adjoint eigenvectors). In an ideal system, i.e. if the number of harmonics is large enough, the FEs should be positioned in the complex plane along vertical lines, i.e. they should be ordered in n groups sharing the same real part, and with imaginary parts whose distance is an integer multiple of $\mathrm{j}\omega_0$ [1]. Because of the truncation error corresponding to the finite value of N_{H}, the FE distributions deviate from the ideal case for large values of the imaginary part. As a general rule, therefore, a wise choice for the better representative FE value appears to concentrate on the eigenvalues whose imaginary part is closer to the real axis [10]. Actually, a more detailed analysis suggests to slightly modify this choice: since all the FE having the same real part differ in the imaginary part of $h\mathrm{j}\omega_0$ for some integer $h \in \mathbb{Z}$, the corresponding frequency domain eigenvectors are (if infinite harmonics are considered) shifted copies one of the other, where the shift takes place in the harmonic index. Therefore, we expect that the more precise eigenvector representation is that whose harmonics run from $-N_{\mathrm{H}}$ to N_{H} (in exponential notation), since all other representatives associated to the same FE are based on frequency components approximated in circulant form (see [22] and (18) below). In other words, since the available FEs are all the possible combinations $\mu_k + h\mathrm{j}\omega_0$ with $k = 1, \ldots, n$ and $h = -N_{\mathrm{H}}, \ldots, N_{\mathrm{H}}$, we look for the n values having $h = 0$, which in turn correspond to those eigenvectors characterized by those harmonic components whose order is symmetrical around DC.

3. The novel approach

The main disadvantage of (11) and (12) is the numerical complexity of the generalized eigenvalue determination, which is $O(N^3)$ [23] (the QZ algorithm is considered here), where $N = n(2N_{\mathrm{H}}+1)$. Since, even for comparatively small circuits, the number of harmonics N_{H} might become large to accurately describe the nonlinear behaviour, the numerical burden rapidly becomes significant.

The idea behind the approach we propose is quite simple: the generalized eigenvalue problems are transformed into standard eigenvalue systems

$$\mu_k \tilde{\boldsymbol{u}}_k = \tilde{\boldsymbol{C}}^{-1}\left[\tilde{\boldsymbol{A}} - \boldsymbol{\Omega}_n \tilde{\boldsymbol{C}}\right]\tilde{\boldsymbol{u}}_k \tag{13}$$

$$\mu_k \tilde{\boldsymbol{v}}_k = \tilde{\boldsymbol{C}}_{\mathrm{T}}^{-1}\left[\tilde{\boldsymbol{A}}_{\mathrm{T}} + \tilde{\boldsymbol{C}}_{\mathrm{T}}\boldsymbol{\Omega}_n\right]\tilde{\boldsymbol{v}}_k, \tag{14}$$

where a direct inspection of the blocks forming $\tilde{\boldsymbol{C}}_{\mathrm{T}}$ (see [20] for details) shows that $\tilde{\boldsymbol{C}}_{\mathrm{T}}^{-1}$ is easily obtained by a proper rearrangement of the blocks constituting $\tilde{\boldsymbol{C}}^{-1}$.

The main advantage of (13) and (14) is of course based on the fact that the direct eigenvalue problem is $O(N^2)$ [23]. The advantage, however, strictly depends on the computation of the system matrix $\tilde{\boldsymbol{C}}^{-1}[\tilde{\boldsymbol{A}} - \boldsymbol{\Omega}_N \tilde{\boldsymbol{C}}]$. Using the gaussian elimination implemented in the LAPACK package [25], we found that this step is in our problems anyway numerically convenient, thus making the transformation advantageous from a numerical standpoint. Fig. 1 shows a comparison in the computation time between the generalized eigenvalue problem (11) and the approach in (13) for the circuit example in Section 4 as a function of the number of harmonics N_{H} (notice that the total size N linearly depends on N_{H}). The results clearly show that, despite the matrix inversion step, the new approach is $O(N^2)$ with respect to the cubic dependence of the generalized eigenvalue problem.

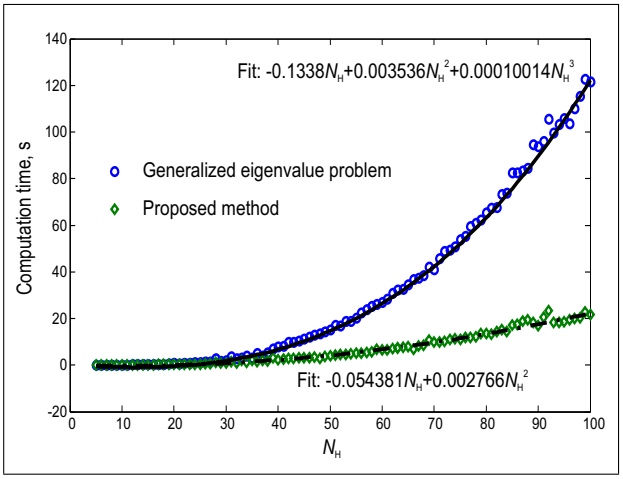

Fig. 1. Computation time (on an Intel Centrino Core2 Duo 2.53 GHz PC running Windows 7 64 bit, MATLAB [24] implementation) of (11) and (13) as a function of N_{H} for the example in Section 4. A polynomial best fit is also shown in the two cases.

On the other hand, a major difficulty is due to the fact that applying to a nonlinear circuit the nodal analysis and linearizing the corresponding DAE around the periodic working point, in general matrix $\boldsymbol{C}(t)$ is not full rank, thus making $\tilde{\boldsymbol{C}}$ not invertible. This problem, however, can be easily circumvented exploiting a trick proposed in [11]: let us consider (11) (the treatment of (12) is fully analogous) and build the modified generalized eigenvalue problem

$$\mu'_k\left[\tilde{\boldsymbol{C}} + \epsilon\left(\tilde{\boldsymbol{A}} - \boldsymbol{\Omega}_n\tilde{\boldsymbol{C}}\right)\right]\tilde{\boldsymbol{u}}'_k = \left[\tilde{\boldsymbol{A}} - \boldsymbol{\Omega}_n\tilde{\boldsymbol{C}}\right]\tilde{\boldsymbol{u}}'_k \tag{15}$$

where ϵ is a properly chosen real number making $\tilde{\boldsymbol{C}} + \epsilon\left(\tilde{\boldsymbol{A}} - \boldsymbol{\Omega}_n\tilde{\boldsymbol{C}}\right)$ invertible: in our experience, a very good choice is $\epsilon = \|\tilde{\boldsymbol{C}}\|_\infty / \|\tilde{\boldsymbol{A}} - \boldsymbol{\Omega}_n\tilde{\boldsymbol{C}}\|_\infty$. Simple calculations allow to verify that the relationship between the solutions of (11) and (15) is

$$\tilde{\boldsymbol{u}}_k = \tilde{\boldsymbol{u}}'_k \qquad \mu_k = \frac{1}{1/\mu'_k - \epsilon} \tag{16}$$

3.1 Problem size minimization

Although the approach in (15) is effective in coping with the $\tilde{\boldsymbol{C}}$ invertibility issue, the numerical efficiency of the Floquet quantities determination still is significantly dependent on the size $N = n(2N_{\mathrm{H}}+1)$ of $\boldsymbol{C}(t)$. This Section introduces a numerical approach entirely based on the

AEÜ Int. J. Electron. Commun.
51 (1997) No. 1, 1–1

HB domain matrices, i.e. avoiding any time-consuming and accuracy-reducing time-frequency conversion, to minimize the size n. Although the algorithm is not in general able to produce a reduced system matrix which is invertible (and, therefore, (15) still needs to be used), the numerical advantage becomes however the more significant the larger is the value of N_{H}.

Linearization of (1) around $\boldsymbol{x}_{\mathrm{S}}(t)$ yields

$$\begin{bmatrix} \boldsymbol{L}_1 \frac{\mathrm{d}\boldsymbol{z}}{\mathrm{d}t} \\ \frac{\mathrm{d}}{\mathrm{d}t}\left(\boldsymbol{J}_{\boldsymbol{f}}(t)\boldsymbol{z}\right) \end{bmatrix} = \begin{bmatrix} \boldsymbol{L}_2\boldsymbol{z} \\ \boldsymbol{J}_{\boldsymbol{g}}(t)\boldsymbol{z} \end{bmatrix} \tag{17}$$

where T-periodic matrices $\boldsymbol{J}_{\boldsymbol{f}}(t)$ and $\boldsymbol{J}_{\boldsymbol{g}}(t)$ are the jacobians of the nonlinear functions $\boldsymbol{f}$ and $\boldsymbol{g}$ calculated in $\boldsymbol{x}_{\mathrm{S}}(t)$. We assume that $\boldsymbol{L}_1$ is full rank: in case of a rank deficient matrix, a reduction procedure such as that proposed below for $\tilde{\boldsymbol{J}}_{\boldsymbol{g},\mathrm{z}}$ can easily be implemented. Notice that since $\boldsymbol{L}_1$ describes the linear part of the circuit, the reduction can take place at the beginning of the simulation, irrespective of the input tone, and is not plagued by the problems related to the time dependency of the kernel of $\boldsymbol{J}_{\boldsymbol{f}}(t)$. We consider explicitly the direct eigenvalue problem only, since the extension to the adjoint system is trivial.

For the sake of simplicity we introduce the discussion assuming a Fourier expansion of the T-periodic matrices in exponential form, although the actual implementation is performed in trigonometric form at the cost of a much more complex notation. This means that $\tilde{\boldsymbol{J}}_{\boldsymbol{f}}$ can be written as a block Toeplitz matrix

$$\tilde{\boldsymbol{J}}_{\boldsymbol{f}} = \begin{bmatrix} \tilde{\boldsymbol{J}}_{\boldsymbol{f}0} & \dots & \tilde{\boldsymbol{J}}_{\boldsymbol{f}2N_{\mathrm{H}}} \\ \vdots & \ddots & \vdots \\ \tilde{\boldsymbol{J}}_{\boldsymbol{f}-2N_{\mathrm{H}}} & \dots & \tilde{\boldsymbol{J}}_{\boldsymbol{f}0} \end{bmatrix} \tag{18}$$

where $\tilde{\boldsymbol{J}}_{\boldsymbol{f}h}$ ($h = -N_{\mathrm{H}}, \dots, N_{\mathrm{H}}$) is the $n \times n$ complex matrix collecting the h-th Fourier coefficient of the elements of $\boldsymbol{J}_{\boldsymbol{f}}(t)$ calculated by the HB solution, and the other terms (i.e. $N_{\mathrm{H}}+1 \leq |h| \leq 2N_{\mathrm{H}}$) are approximated according to the block circulant structure in [22]. Furthermore, the time derivative operator $\boldsymbol{\Omega}$ is a complex, diagonal matrix of size $2N_{\mathrm{H}}+1$.

The first step is the application of the null space decomposition (NSD) algorithm presented in Appendix A1.1 to $\boldsymbol{J}_{\boldsymbol{f}}(t)$, identifying a unitary matrix $\boldsymbol{H}$ able to single out the kernel of $\boldsymbol{J}_{\boldsymbol{f}}(t)$. Notice that, although the rank of $\boldsymbol{J}_{\boldsymbol{f}}(t)$ is assumed constant, the kernel (i.e., the rows of the unitary matrix identifying the kernel of the matrix) is in general time varying: in order to be able to allow for an algorithm completely in the HB domain, we need a constant matrix $\boldsymbol{H}$ and therefore we have devised the algorithm in Appendix A2 to determine a constant matrix $\boldsymbol{Z}_{\perp}$ extracting the constant part of the nullspace of $\boldsymbol{J}_{\boldsymbol{f}}(t)$. Since the total NSD transformation is unitary, its rows must span the entire $\mathbb{R}^{n-m}$. Therefore we can easily build a constant unitary matrix $\boldsymbol{H}$ such that

$$\boldsymbol{H}\boldsymbol{J}_{\boldsymbol{f}}(t) = \begin{bmatrix} \boldsymbol{K} \\ \boldsymbol{Z}_{\perp} \end{bmatrix} \boldsymbol{J}_{\boldsymbol{f}}(t) = \begin{bmatrix} \boldsymbol{J}_{\boldsymbol{f},\mathrm{nz}}(t) \\ \boldsymbol{0}_{(n-m-\rho_{\perp})\times n} \end{bmatrix} \tag{19}$$

where $\boldsymbol{K} \in \mathbb{R}^{\rho_{\perp}\times n}$ and $\boldsymbol{Z}_{\perp} \in \mathbb{R}^{(n-m-\rho_{\perp})\times n}$ are pseudo-unitary matrices, $\rho_{\perp}$ is the size of the time-invariant part of the kernel of $\boldsymbol{J}_{\boldsymbol{f}}(t)$, and $\boldsymbol{0}_{p\times q}$ is the zero matrix of size $p \times q$. $\boldsymbol{K}$ is assembled choosing, through a standard orthonormalization procedure, $\rho_{\perp}$ normalized vectors which, together with the rows of $\boldsymbol{Z}_{\perp}$, span $\mathbb{R}^{n-m}$. Since $\boldsymbol{Z}_{\perp}$ contains only the time invariant part of the nullspace of $\boldsymbol{J}_{\boldsymbol{f}}(t)$, $\boldsymbol{J}_{\boldsymbol{f},\mathrm{nz}}(t)$ is not guaranteed to be invertible (unless $\rho_{\perp} = \rho$), thus leading to a noninvertible reduced system matrix that needs to be regularized as in (15).

Since $\boldsymbol{H}$ is independent of t (as well as $\boldsymbol{L}_1$ and $\boldsymbol{L}_2$), the frequency transformed version $\tilde{\boldsymbol{H}} \in \mathbb{R}^{(n-m)(2N_{\mathrm{H}}+1)\times n(2N_{\mathrm{H}}+1)}$ is block diagonal, and therefore commutes with the (block diagonal) time derivative operator $\boldsymbol{\Omega}_{n-m}$. Using the Floquet ansatz $\boldsymbol{z}(t) = \exp(\mu_k t)\boldsymbol{u}_k(t)$, in frequency domain (17) becomes

$$\left(\mu_k \boldsymbol{I}_{n(2N_{\mathrm{H}}+1)} + \boldsymbol{\Omega}_n\right) \begin{bmatrix} \tilde{\boldsymbol{L}}_1 \\ \tilde{\boldsymbol{H}}\tilde{\boldsymbol{J}}_{\boldsymbol{f}} \end{bmatrix} \tilde{\boldsymbol{u}}_k = \begin{bmatrix} \tilde{\boldsymbol{L}}_2 \\ \tilde{\boldsymbol{H}}\tilde{\boldsymbol{J}}_{\boldsymbol{g}} \end{bmatrix} \tilde{\boldsymbol{u}}_k \tag{20}$$

where $\boldsymbol{I}_{n(2N_{\mathrm{H}}+1)}$ is the identity matrix of size $n(2N_{\mathrm{H}}+1)$, and

$$\tilde{\boldsymbol{H}}\tilde{\boldsymbol{J}}_{\boldsymbol{f}} = \begin{bmatrix} \tilde{\boldsymbol{J}}_{\boldsymbol{f},\mathrm{nz}} \\ \boldsymbol{0}_{(n-m-\rho_{\perp})(2N_{\mathrm{H}}+1)\times n(2N_{\mathrm{H}}+1)} \end{bmatrix} \tag{21}$$

and $\tilde{\boldsymbol{J}}_{\boldsymbol{f},\mathrm{nz}}$ has size $\rho_{\perp}(2N_{\mathrm{H}}+1) \times n(2N_{\mathrm{H}}+1)$. We now focus on the last $(n-m-\rho_{\perp})(2N_{\mathrm{H}}+1)$ rows of $\tilde{\boldsymbol{H}}\tilde{\boldsymbol{J}}_{\boldsymbol{g}}$, denoted as $\tilde{\boldsymbol{J}}_{\boldsymbol{g},\mathrm{z}}$:

$$\tilde{\boldsymbol{H}}\tilde{\boldsymbol{J}}_{\boldsymbol{g}} = \begin{bmatrix} \tilde{\boldsymbol{J}}_{\boldsymbol{g},\mathrm{nz}} \\ \tilde{\boldsymbol{J}}_{\boldsymbol{g},\mathrm{z}} \end{bmatrix}. \tag{22}$$

Because of (21)

$$\tilde{\boldsymbol{J}}_{\boldsymbol{g},\mathrm{z}}\tilde{\boldsymbol{u}}_k = \boldsymbol{0}, \tag{23}$$

therefore the size of (20) can be reduced eliminating $(n-m-\rho_{\perp})(2N_{\mathrm{H}}+1)$ real equations. Notice that for (20) to be consistent, $\tilde{\boldsymbol{J}}_{\boldsymbol{g},\mathrm{z}}$ should be full rank.

In order to make use of the rectangular linear system (23), we should be able to extract an invertible submatrix of $\tilde{\boldsymbol{J}}_{\boldsymbol{g},\mathrm{z}}$, e.g. by applying the reduced row echelon form (RREF) algorithm in Appendix A1.2. A direct application of RREF would however be numerically very intensive, because of the size of $\tilde{\boldsymbol{J}}_{\boldsymbol{g},\mathrm{z}}$, especially if a large N_{H} is used. We propose here a heuristical approach, which in our experience has been proven to be very effective: consider the real and positive $(n-m-\rho_{\perp})\times n$ matrix $\tilde{\boldsymbol{J}}_{\boldsymbol{g},\mathrm{e}}$ obtained by summing on the harmonic index the square magnitude of the elements of $\tilde{\boldsymbol{J}}_{\boldsymbol{g},\mathrm{z}}$, which can be easily and quickly assembled. Because of Parseval identity, this corresponds to the collection of the energy of each element of $\boldsymbol{Z}_{\perp}\boldsymbol{J}_{\boldsymbol{g}}(t)$. The RREF algorithm is then applied to $\tilde{\boldsymbol{J}}_{\boldsymbol{g},\mathrm{e}}$, obtaining the pivoting set $j_{\tilde{J}_{g,\mathrm{e}}}$ and its complement $\bar{j}_{\tilde{J}_{g,\mathrm{e}}}$ leading to the partition (and pivoting) of $\tilde{\boldsymbol{J}}_{\boldsymbol{g},\mathrm{z}}$ into

$$\begin{bmatrix} \tilde{\boldsymbol{J}}_{\boldsymbol{g},\mathrm{z}1} & \tilde{\boldsymbol{J}}_{\boldsymbol{g},\mathrm{z}2} \end{bmatrix} \tag{24}$$

where $\tilde{\boldsymbol{J}}_{\boldsymbol{g},\mathrm{z1}} = \tilde{\boldsymbol{J}}_{\boldsymbol{g},\mathrm{z}}(:, \bar{j}_{\tilde{j}_{g,\mathrm{e}}})$ ($(n-m-\rho_\perp)(2N_\mathrm{H}+1) \times (m+\rho_\perp)(2N_\mathrm{H}+1)$), i.e. the collection of columns of $\tilde{\boldsymbol{J}}_{\boldsymbol{g},\mathrm{z}}$ corresponding to the set $\bar{j}_{\tilde{j}_{g,\mathrm{e}}}$ where the choice of the columns should be intended implemented as applied to the harmonic blocks ordered as in (18). Matrix $\tilde{\boldsymbol{J}}_{\boldsymbol{g},\mathrm{z2}} = \tilde{\boldsymbol{J}}_{\boldsymbol{g},\mathrm{z}}(:, j_{\tilde{j}_{g,\mathrm{e}}})$ ($(m+\rho_\perp)(2N_\mathrm{H}+1) \times (m+\rho_\perp)(2N_\mathrm{H}+1)$) is, if the pivoting vector is well chosen, invertible. Therefore, the quality of the pivoting vector is verified by checking the condition number of $\tilde{\boldsymbol{J}}_{\boldsymbol{g},\mathrm{z2}}$.

Applying the pivoting operation also to the unknown vector

$$\tilde{\boldsymbol{u}}_k \rightarrow \begin{bmatrix} \tilde{\boldsymbol{u}}_{k,1} \\ \tilde{\boldsymbol{u}}_{k,2} \end{bmatrix} = \begin{bmatrix} \tilde{\boldsymbol{u}}_k(\bar{j}_{\tilde{j}_{g,\mathrm{e}}}) \\ \tilde{\boldsymbol{u}}_k(j_{\tilde{j}_{g,\mathrm{e}}}) \end{bmatrix}, \tag{25}$$

from (23) follows

$$\tilde{\boldsymbol{u}}_{k,2} = -\tilde{\boldsymbol{J}}_{\boldsymbol{g},\mathrm{z2}}^{-1} \tilde{\boldsymbol{J}}_{\boldsymbol{g},\mathrm{z1}} \tilde{\boldsymbol{u}}_{k,1}, \tag{26}$$

i.e. the number of real unknowns is reduced to $(m+\rho_\perp)(2N_\mathrm{H}+1)$, the size of $\tilde{\boldsymbol{u}}_{k,1}$. Making use of (26) into (20), a system like (11) of size $(m+\rho_\perp)(2N_\mathrm{H}+1)$ is obtained, where

$$\tilde{\boldsymbol{C}} = \begin{bmatrix} \tilde{\boldsymbol{L}}_{1,1} - \tilde{\boldsymbol{L}}_{1,2} \tilde{\boldsymbol{J}}_{\boldsymbol{g},\mathrm{z2}}^{-1} \tilde{\boldsymbol{J}}_{\boldsymbol{g},\mathrm{z1}} \\ \tilde{\boldsymbol{J}}_{\boldsymbol{f},\mathrm{nz1}} - \tilde{\boldsymbol{J}}_{\boldsymbol{f},\mathrm{nz2}} \tilde{\boldsymbol{J}}_{\boldsymbol{g},\mathrm{z2}}^{-1} \tilde{\boldsymbol{J}}_{\boldsymbol{g},\mathrm{z1}} \end{bmatrix} \tag{27}$$

$$\tilde{\boldsymbol{A}} = \begin{bmatrix} \tilde{\boldsymbol{L}}_{2,1} - \tilde{\boldsymbol{L}}_{2,2} \tilde{\boldsymbol{J}}_{\boldsymbol{g},\mathrm{z2}}^{-1} \tilde{\boldsymbol{J}}_{\boldsymbol{g},\mathrm{z1}} \\ \tilde{\boldsymbol{J}}_{\boldsymbol{g},\mathrm{nz1}} - \tilde{\boldsymbol{J}}_{\boldsymbol{g},\mathrm{nz2}} \tilde{\boldsymbol{J}}_{\boldsymbol{g},\mathrm{z2}}^{-1} \tilde{\boldsymbol{J}}_{\boldsymbol{g},\mathrm{z1}} \end{bmatrix} \tag{28}$$

and the unknown vector is $\tilde{\boldsymbol{u}}_{k,1}$. In the previous equations, matrices $\tilde{\boldsymbol{L}}_{1,q}$, $\tilde{\boldsymbol{L}}_{2,q}$, $\tilde{\boldsymbol{J}}_{\boldsymbol{g},\mathrm{nz}q}$ and $\tilde{\boldsymbol{J}}_{\boldsymbol{f},\mathrm{nz}q}$ ($q = 1, 2$) are defined through the application of the pivoting set to the corresponding original matrices. Notice that if $\rho_\perp$ is equal to the rank of $\boldsymbol{J}_{\boldsymbol{f}}(t)$, i.e. if the kernel of $\boldsymbol{J}_{\boldsymbol{f}}(t)$ is independent of time, the matrix defined in (27) is full rank.

3.2 Summary of the algorithm

For the sake of clarity, we summarize here the steps of the proposed algorithm, pointing out the sequence of actions to be implemented:

1. assemble the full circuit equations according to the generalized nodal approach;
2. minimize matrix $\boldsymbol{L}_1$ representing the linear part of the circuit making it full rank. This step is to be performed once (since matrix is constant) by applying the RREF algorithm;
3. determine the circuit time-periodic working point $\boldsymbol{x}_\mathrm{S}(t)$ by means of the HB technique;
4. minimize the size of the $\boldsymbol{J}_{\boldsymbol{f}}(t)$ jabobian exploiting the algorithm in Section 3.1;
5. if the kernel of $\boldsymbol{J}_{\boldsymbol{f}}(t)$ is not full rank, apply (15) checking the condition number of the obtained modified matrix;
6. calculate the Floquet quantities exploiting (13) and (14).

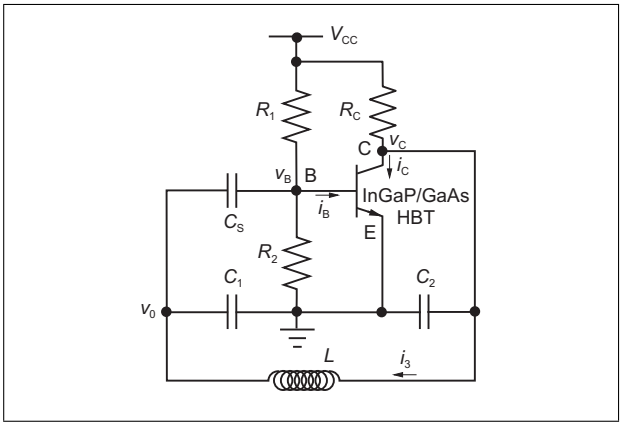

Fig. 2. Circuit of the Colpitts oscillator.

4. Example

As an example of application we consider the Colpitts oscillator in Fig. 2. The transistor is the InGaP/GaAs HBT described by the Gummell Poon model in [26], including device nonlinear capacitances and parasitic effects. The circuit parameters are: $V_\mathrm{CC} = 6$ V, $R_1 = 10$ kΩ, $R_2 = 4.2$ kΩ, $R_\mathrm{C} = 300$ Ω, $C_1 = 5$ pF, $C_2 = 5$ pF, $C_\mathrm{S} = 1$ μF and $L = 10$ nH. As shown in [8], the oscillation frequency obtained through a HB simulation with $N_\mathrm{H} = 300$ is 0.994 GHz.

After the reduction of the linear part of the circuit system matrix, the number of unknowns is $n = 9$, leading to a size of the HB Floquet problem equal to $n(2N_\mathrm{H}+1) = 5409$. Applying the NSD to $\boldsymbol{J}_{\boldsymbol{f}}(t)$, the nullspace is found to have size 4 (which means that the LPTV system has 4 FEs equal to $-\infty$). Two of the elements of the orthonormal base of the kernel of $\boldsymbol{J}_{\boldsymbol{f}}(t)$ are constant, while for the other two a time dependent rotation is observed, as shown in Fig. 3: this means that $\rho_\perp = 2$. Therefore, the application of the reduction procedure described in Section 3.1 leads to the problem size $7(2N_\mathrm{H}+1) = 4207$, i.e. a 22% reduction.

The results of the application of the previous method, based on the solution of a generalized eigenvalue problem, and of the algorithm proposed in this work are summarized in Table 1, where the Floquet eigenvalues are compared. Notice that the table lists 5 FEs only, since the partial reduction of the system due to the nonconstant nullspace still leaves 2 FEs equal to $-\infty$. The first eigenvalue μ_1 is associated to the tangent vector to the oscillator solution, and in principle should be zero. As well known in the literature [27], the numerical accuracy of its determination is very poor: as usual, the proper eigenvalue is chosen by looking for the direct eigenvector that better approximates the orthogonality condition with the corresponding adjoint eigenvector $\boldsymbol{v}_1(t) = \dot{\boldsymbol{x}}_\mathrm{S}(t)$ [20]. Applying the same error estimation procedure in [20], the other FEs result well approximated up to the fifth digit. The complex FE μ_4 appears without the corresponding complex conjugate value because the imaginary part is equal to $\omega_0/2$, and therefore is mapped onto a real FM.

AEÜ Int. J. Electron. Commun.
51 (1997) No. 1, 1–1

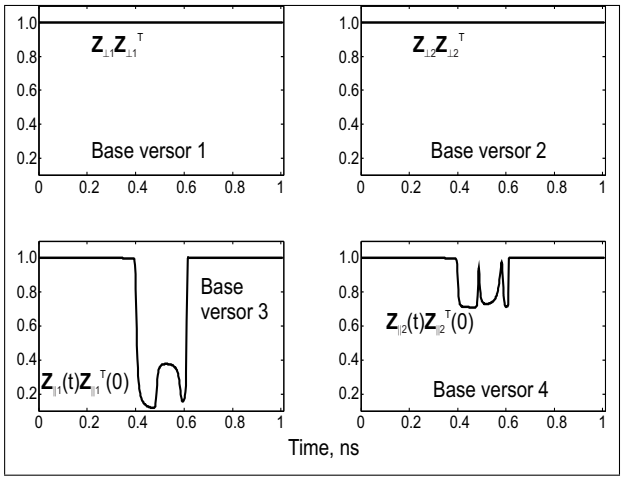

Fig. 3. Time-dependence (over one period) of the orthonormal base elements $\boldsymbol{Z}_{\|j}(t)$ and $\boldsymbol{Z}_{\perp j}(t)$ (the j-th row of the corresponding matrix in (A5)) projected along the corresponding value for $t = 0$ for the nullspace of $\boldsymbol{J_f}(t)$ as found by the NSD algorithm.

Table 1. Comparison between the generalized eigenvalue and the simple eigenvalue methodologies. MATLAB [24] implementation on an Intel Centrino Core2 Duo 2.53 GHz PC running Windows 7 64 bit.

	Previous method	This work
Time	1816 s	148 s
μ_1	-473760.9482	-473761.6942
μ_2	-1158.8725	-1158.8808
μ_3	-2237488716.6516	-2237491363.8365
μ_4	$-3222824027.1933+$ 3124059245.1654j	$-3222819597.1577+$ 3124060182.7958j
μ_5	$-4.36927537 \times 10^{12}$	$-4.37020515 \times 10^{12}$

The computation time for the generalized eigenvalue problem is measured on the full system (i.e., no reduction of the system size is performed), while for the present approach the entire computation is taken into account (i.e., both the system reduction and the determination of the FEs). Comparing the results of the two methods, the accuracy of the new approach appears excellent, whereas the computation time is improved by one order of magnitude.

5. Conclusion

We have presented an algorithm for the computation of all the Floquet quantities relevant for important assessments of the operation of nonlinear circuits working in time-periodic conditions. The method can be applied to both forced and autonomous systems, and is entirely based on the HB technique. In particular, all the matrix transformations are entirely taking place in the spectral domain, thus avoiding time intensive DFT operations which, on the other hand, may also imply a degradation of the numerical accuracy.

The application of the algorithm shows that an important improvement of the computation time of one order of magnitude with respect to previous approaches is observed, without any significant reduction in the precision of the calculated Floquet quantities.

Appendix

A1. Matrix manipulation tools

We briefly describe in this Section the relevant properties of two matrix manipulation tools that we use in the implementation of Floquet analysis, the *null space decomposition* (NSD) and the *reduced row echelon form* (RREF) [28, 29]. To fix the ideas, let us consider a matrix $\boldsymbol{M} \in \mathbb{R}^{m\times n}$ ($m \leq n$) of rank $\rho \leq m$.

A1.1 Null space decomposition

We consider here a matrix linear transformation that allows to identify the kernel of $\boldsymbol{M}$. A unitary matrix $\boldsymbol{H} \in \mathbb{R}^{m\times m}$ exists (i.e., $\boldsymbol{H}\boldsymbol{H}^{\mathrm{T}} = \boldsymbol{H}^{\mathrm{T}}\boldsymbol{H} = \boldsymbol{I}_m$ where $\boldsymbol{I}_m$ is the identity matrix of size m) such that [28, 29]

$$\boldsymbol{H}\boldsymbol{M} = \begin{bmatrix} \boldsymbol{M}_{\mathrm{nz}} \\ \boldsymbol{0}_{(m-\rho)\times m} \end{bmatrix} \tag{A1}$$

where $\boldsymbol{0}_{p,q}$ is a null matrix of size $p \times q$ and $\boldsymbol{M}_{\mathrm{nz}} \in \mathbb{R}^{\rho\times n}$ has rank ρ. Matrix $\boldsymbol{H}$ is decomposed into two submatrices

$$\boldsymbol{H} = \begin{bmatrix} \boldsymbol{K} \\ \boldsymbol{Z} \end{bmatrix} \tag{A2}$$

where $\boldsymbol{K} \in \mathbb{R}^{\rho\times m}$ and $\boldsymbol{Z} \in \mathbb{R}^{(m-\rho)\times m}$, whose rows represent, respectively, a basis for the orthogonal part and for the kernel of $\boldsymbol{M}$.

The NSD is a particular case of orthogonal decomposition [29] allowing to define a matrix which singles out the full rank part of $\boldsymbol{M}$. Many implementations for this operation are possible, e.g. the Householder transformation [28, 29]. In our experience, an effective solution is to implement (A1) exploiting the QR decomposition [29], using the variant of the QR algorithm returning an upper triangular matrix whose diagonal terms are (in magnitude) in decreasing order.

Notice that the NSD matrix is not unique. In fact, given a unitary matrix $\boldsymbol{Q}$ partitioned as

$$\boldsymbol{Q} = \begin{bmatrix} \boldsymbol{Q}_{11} & \boldsymbol{Q}_{12} \\ \boldsymbol{0}_{m-\rho\times\rho} & \boldsymbol{Q}_{22} \end{bmatrix} \tag{A3}$$

where $\boldsymbol{Q}_{11}$ and $\boldsymbol{Q}_{22}$ are square matrices of size $\rho \times \rho$ and $(m-\rho)\times(m-\rho)$, respectively, $\boldsymbol{H}' = \boldsymbol{Q}\boldsymbol{H}$ still satisfies (A1) (of course with a different $\boldsymbol{M}_{\mathrm{nz}}$).

A1.2 Reduced row echelon form

The RREF is a reduction technique based on a pivoting strategy, typically used for the solution of linear systems

with non-full rank (or, in general, with a rectangular system matrix). The RREF $\boldsymbol{P}$ of $\boldsymbol{M}$ has two important features [29]: the last $m-\rho$ rows of $\boldsymbol{P}$ are zero, and for each row of $\boldsymbol{P}$ the position of the first non-null element (starting from left) is the row pivot. We collect all the pivots in the set j_M, which has the following properties [29]:

1. j_M has ρ elements
2. j_M defines a basis for the space spanned by $\boldsymbol{M}$, meaning that

$$\text{span}\left\{\{\boldsymbol{M}(:,j)\}_{j=1}^{n}\right\} = \text{span}\left\{\{\boldsymbol{M}(:,j_M(j))\}_{j=1}^{\rho}\right\}$$

where $\boldsymbol{M}(:,j)$ is the j-th column of $\boldsymbol{M}$. We make use of the pivoting vector j_M (i.e., we do not require the full $\boldsymbol{P}$), and of its complement $\bar{j}_M = \{1,\ldots,n\} \setminus j_M$. According to our experience the best selection approach is based again on the QR factorization [29] returning an upper triangular matrix whose diagonal terms are (in magnitude) in decreasing order.

A2. Determination of the constant part of the kernel of a periodic matrix

Let us consider a T periodic matrix $\boldsymbol{M}(t) \in \mathbb{R}^{m\times n}$, where $m \le n$. For the sake of simplicity, we exploit the exponential form of Fourier series and order the collection of harmonic components as in (18). Let us denote as $\tilde{\boldsymbol{M}}_h$ the $m \times n$ complex matrix representing the h-th Fourier component of $\boldsymbol{M}(t)$.

Theorem 1 Let $\boldsymbol{M}(t) \in \mathbb{R}^{m\times n}$ $(m \le n)$ with rank ρ indepedent of time (thus, the size $m-\rho$ of the kernel of $\boldsymbol{M}(t)$ is independent of time), whose Fourier representation is ordered as in (18). Let $\boldsymbol{Z}_\perp \in \mathbb{R}^{m-\rho_\perp\times m}$ $(\rho_\perp \ge \rho)$ be the constant part of the nullspace of $\boldsymbol{M}(t)$. Then

$$\boldsymbol{Z}_\perp \tilde{\boldsymbol{M}}_h = \boldsymbol{0}_{m-\rho_\perp\times n} \quad \forall h \in \mathbb{Z}.$$

□

Proof: Since the rank of $\boldsymbol{M}(t)$ is constant, it is possible to find a unitary matrix $\boldsymbol{H}(t) = [\boldsymbol{K}^{\mathrm{T}}(t), \boldsymbol{Z}^{\mathrm{T}}(t)]^{\mathrm{T}}$ such that (A1) holds, e.g. using the NSD algorithm in Appendix A1.1. As noted in Appendix A1.1, $\boldsymbol{H}$ is not uniquely defined since it can be transformed into another unitary matrix $\boldsymbol{H}'(t)$ using $\boldsymbol{H}' = \boldsymbol{Q}\boldsymbol{H}$, where $\boldsymbol{Q}$ is again a unitary transformation as in (A3). Therefore, if a nontrivial constant part of the nullspace of $\boldsymbol{M}(t)$ exists, a unitary transformation $\boldsymbol{Q}_{22}(t)$ exists such that

$$\boldsymbol{Q}_{22}(t)\boldsymbol{Z}(t) = \begin{bmatrix}\boldsymbol{Z}_\parallel(t)\\ \boldsymbol{Z}_\perp\end{bmatrix} \tag{A4}$$

where $\boldsymbol{Z}_\perp \in \mathbb{R}^{m-\rho_\perp\times m}$ is constant and $\boldsymbol{Z}_\parallel(t) \in \mathbb{R}^{\rho_\perp-\rho\times m}$. Since $\boldsymbol{H}$ is unitary, $\boldsymbol{Z}$ is pseudo-unitary (i.e., $\boldsymbol{Z}\boldsymbol{Z}^{\mathrm{T}} = \boldsymbol{I}_{m-\rho}$) as well as $\boldsymbol{Z}_\perp$ and $\boldsymbol{Z}_\parallel$, which are also pseudo-orthogonal ($\boldsymbol{Z}_\perp\boldsymbol{Z}_\parallel^{\mathrm{T}} = \boldsymbol{0}$ and $\boldsymbol{Z}_\parallel\boldsymbol{Z}_\perp^{\mathrm{T}} = \boldsymbol{0}$). In other words, a unitary transformation $\boldsymbol{H}'(t)$ exists such that

$$\begin{bmatrix}\boldsymbol{K}'(t)\\ \boldsymbol{Z}_\parallel(t)\\ \boldsymbol{Z}_\perp\end{bmatrix}\boldsymbol{M}(t) = \begin{bmatrix}\boldsymbol{M}_{\text{nz}}(t)\\ \boldsymbol{0}\\ \boldsymbol{0}\end{bmatrix}. \tag{A5}$$

Expressing (A5) in frequency domain we find

$$\begin{bmatrix}\tilde{\boldsymbol{K}}'\\ \tilde{\boldsymbol{Z}}_\parallel\\ \tilde{\boldsymbol{Z}}_\perp\end{bmatrix}\tilde{\boldsymbol{M}} = \begin{bmatrix}\tilde{\boldsymbol{M}}_{\text{nz}}\\ \boldsymbol{0}\\ \boldsymbol{0}\end{bmatrix} \tag{A6}$$

where, since $\boldsymbol{Z}_\perp$ is constant, $\tilde{\boldsymbol{Z}}_\perp$ is block diagonal where each diagonal block is $\boldsymbol{Z}_\perp$. Therefore, the lower third part of (A6) yields the required result. □

Based on Theorem 1 we propose an algorithm able to quickly recover $\boldsymbol{Z}_\perp$ starting from the Fourier components $\tilde{\boldsymbol{M}}_h$. Let us denote as $\boldsymbol{H}_h = [\boldsymbol{K}_h^{\mathrm{T}}, \boldsymbol{Z}_h^{\mathrm{T}}]^{\mathrm{T}}$ (the size of $\boldsymbol{Z}_h$ is $m-\rho_h \times n$) the result of the NSD applied to $\tilde{\boldsymbol{M}}_h$, so that because of Theorem 1 a unitary $\boldsymbol{U}_h$ (size $m-\rho_h\times m-\rho_h$) exists such that $\boldsymbol{U}_h\boldsymbol{Z}_h = [\boldsymbol{Z}_{\parallel,h}^{\mathrm{T}}, \boldsymbol{Z}_\perp^{\mathrm{T}}]^{\mathrm{T}}$. We proceed as follows:

1. calculate $\boldsymbol{Z}_0$ and $\boldsymbol{Z}_1$;
2. calculate the singular value decomposition (SVD) [29] of $\boldsymbol{Z}_0\boldsymbol{Z}_1^{\mathrm{T}}$, i.e. find the unitary matrices $\boldsymbol{S}_{01}$ $(m-\rho_0 \times m-\rho_0)$ and $\boldsymbol{D}_{01}$ $(m-\rho_1 \times m-\rho_1)$ such that
$$\boldsymbol{Z}_0\boldsymbol{Z}_1^{\mathrm{T}} = \boldsymbol{S}_{01}\boldsymbol{V}_{01}\boldsymbol{D}_{01}$$
where $\boldsymbol{V}_{01}$ $(m-\rho_0 \times m-\rho_1)$ is diagonal;
3. choose the rows of $\boldsymbol{Z}_\perp$ as the rows of $\boldsymbol{S}_{01}^{\mathrm{T}}\boldsymbol{Z}_0$ that, multiplied times $\boldsymbol{Z}_1^{\mathrm{T}}\boldsymbol{D}_{01}^{\mathrm{T}}$, yield $[0,\ldots,0,1,0,\ldots,0]$ as a result (where the 1 is in j-th position in the vector where $j = 1,\ldots,\rho_\perp$);
4. repeat the previous steps with $\boldsymbol{Z}_0$ and $\boldsymbol{Z}_2$ to verify the numerical precision of the determined $\boldsymbol{Z}_\perp$.

The consistency of step 3 can be easily verified decomposing

$$\boldsymbol{S}_{01}^{\mathrm{T}}\boldsymbol{Z}_0 = \begin{bmatrix}\boldsymbol{S}_{01,\text{nz}}^{\mathrm{T}}\boldsymbol{Z}_{0,\text{nz}}\\ \boldsymbol{Z}_\perp\end{bmatrix} \quad \boldsymbol{D}_{01}\boldsymbol{Z}_1 = \begin{bmatrix}\boldsymbol{D}_{01,\text{nz}}\boldsymbol{Z}_{1,\text{nz}}\\ \boldsymbol{Z}_\perp\end{bmatrix} \tag{A7}$$

where $\boldsymbol{S}_{01,\text{nz}}$ and $\boldsymbol{D}_{01,\text{nz}}$ are the unitary matrices of the SVD of $\boldsymbol{Z}_{0,\text{nz}}\boldsymbol{Z}_{1,\text{nz}}$. In fact, from (A7) follows

$$\begin{aligned}\boldsymbol{S}_{01}^{\mathrm{T}}\boldsymbol{Z}_0\boldsymbol{Z}_1^{\mathrm{T}}\boldsymbol{D}_{01}^{\mathrm{T}} &= \\ &= \begin{bmatrix}\boldsymbol{S}_{01,\text{nz}}^{\mathrm{T}}\boldsymbol{Z}_{0,\text{nz}}\boldsymbol{Z}_{1,\text{nz}}\boldsymbol{D}_{01,\text{nz}} & \boldsymbol{S}_{01,\text{nz}}^{\mathrm{T}}\boldsymbol{Z}_{0,\text{nz}}\boldsymbol{Z}_\perp^{\mathrm{T}}\\ \boldsymbol{Z}_\perp\boldsymbol{Z}_{1,\text{nz}}\boldsymbol{D}_{01,\text{nz}} & \boldsymbol{Z}_\perp\boldsymbol{Z}_\perp^{\mathrm{T}}\end{bmatrix}\\ &= \begin{bmatrix}\boldsymbol{V}_{01,\text{nz}} & \boldsymbol{0}_{(m-\rho_0-\rho_\perp)\times\rho_\perp}\\ \boldsymbol{0}_{\rho_\perp\times(m-\rho_1-\rho_\perp)} & \boldsymbol{I}_{\rho_\perp}\end{bmatrix}.\end{aligned}$$

References

[1] Farkas, M.: Periodic motions. New York: Springer-Verlag, 1994.

[2] Guckenheimer, J.; Holmes, P.: Nonlinear oscillations, dynamical systems, and bifurcations of vector fields. New York: Springer-Verlag, 1983.

[3] Demir, A.; Mehrotra, A.; Roychowdhury, J.: Phase noise in oscillators: A unifying theory and numerical methods for characterization. IEEE Trans. Circuits Syst. I, Fundam. Theory Appl. **57** (May 2000), 655–674.

[4] Demir, A.: Phase noise and timing jitter in oscillators with colored-noise sources. IEEE Trans. Circuits Syst. I, Fundam. Theory Appl. **49** (December 2002), 1782–1791.

[5] Srivastava, S.; Roychowdhury, J.: Analytical equations for nonlinear phase errors and jitter in ring oscillators. IEEE Trans. Circuits Syst. I, Regul. Pap. **54** (October 2007), 2321–2329.

[6] Carbone, A.; Palma, F.: Considering noise orbital deviations on the evaluation of power density spectrum of oscillators. IEEE Trans. Circuits Syst. Express Briefs **53** (June 2006), 438–442.

[7] Traversa, F.; Bonani, F.: Asymptotic stochastic characterization of phase and amplitude noise in free-running oscillators. Fluctuation Noise Lett. (2011). accepted for publication.

[8] Traversa, F.; Bonani, F.: Oscillator noise: a nonlinear perturbative theory including orbital fluctuations and phase-orbital correlation. IEEE Trans. Circuits Syst. I, Regul. Pap. (2011). Accepted for publication.

[9] Lust, K.: Improved numerical Floquet multipliers. Int. J. Bifurcation Chaos **11** (September 2001), 2389–2410.

[10] Traversa, F.; Bonani, F.; Donati Guerrieri, S.: A frequency-domain approach to the analysis of stability and bifurcations in nonlinear systems described by differential-algebraic equations. Int. J. Circuit Theory Appl. **36** (2004), 421–439.

[11] Brambilla, A.; Gruosso, G.; Storti Gajani, G.: Determination of floquet exponents for small-signal analysis of nonlinear periodic circuits. IEEE Trans. Computer-Aided Design Integr. Circuits Syst. **28** (March 2009), 447–451.

[12] Traversa, F.; Cappelluti, F.; Bonani, F.; Ghione, G.: Assessment of thermal instabilities and oscillations in multifinger heterojunction bipolar transistors through a harmonic-balance-based CAD-oriented dynamic stability analysis technique. IEEE Trans. Microw. Theory Tech. **57** (December 2009), 3461–3468.

[13] Cappelluti, F.; Traversa, F.; Bonani, F.; Donati Guerrieri, S.; Ghione, G.: Rigorous, HB-based nonlinear stability analysis of multi-device power amplifier. European Microwave Integrated Circuits Conference, Paris, France, 2010. 90–93.

[14] Demir, A.: Floquet theory and non-linear perturbation analysis for oscillators with differential-algebraic equations. Int. J. Circuit Theory Appl. **28** (2000), 163–185.

[15] Kundert, K.; Sangiovanni-Vincentelli, A.; White, J.: Steady-state methods for simulating analog and microwave circuits. Boston: Kluwer Academic Publisher, 1990.

[16] Kuznetsov, Y.: Elements of applied bifurcation theory. Second ed. New York: Springer-Verlag, 1998.

[17] Brambilla, A.; Storti Gajani, G.: Computation of all Floquet eigenfunctions in autonomous circuits. Int. J. Circuit Theory Appl. **36** (2008), 717–737.

[18] Kundert, K.: Introduction to RF simulation and its application. IEEE J. Solid-State Circuits **34** (September 1999), 1298–1319.

[19] Rizzoli, V.; Masotti, D.; Mastri, F.; Montanari, E.: System-oriented harmonic-balance algorithms for circuit-level simulation. IEEE Trans. Computer-Aided Design Integr. Circuits Syst. **30** (February 2011), 256–269.

[20] Traversa, F.; Bonani, F.: Frequency domain evaluation of the adjoint Floquet eigenvectors for oscillator noise characterization. IET Circuits Devices Syst. **5** (2011), 46–51.

[21] Feldmann, P.; Melville, R.; Long, D.: Efficient frequency domain analysis of large nonlinear analog circuits. IEEE Custom Integrated Circuits Conference, 1996. 461–464.

[22] Roychowdhury, J.; Long, D.; Feldmann, P.: Cyclostationary noise analysis of large RF circuits with multitone excitations. IEEE J. Solid-State Circuits **33** (March 1998), 324–336.

[23] Golub, G.; van Loan, C.: Matrix computations. Third ed. Baltimore: The Johns Hopkins University Press, 1996.

[24] The Mathworks Inc.: Matlab version r2010b. 2010.

[25] LAPACK – Linear Algebra Package. 2010. http://www.netlib.org/lapack/.

[26] Sweet, A. A.: Designing bipolar transistor radio frequency integrated circuits. Norwood: Artech House, 2008.

[27] Demir, A.; Roychowdhury, J.: A reliable and efficient procedure for oscillator ppv computation, with phase noise macromodeling applications. IEEE Trans. Computer-Aided Design Integr. Circuits Syst. **22** (February 2003), 188–197.

[28] Stoer, J.; Bulirsch, R.: Introduction to numerical analysis. Third ed. New York: Springer-Verlag, 2002.

[29] Meyer, C.: Matrix analysis and applied linear algebra. SIAM: Society for Industrial and Applied Mathematics, 2000.

Fabio L. Traversa was born in Bari, Italy, in 1979. He received the Laurea degree in Nuclear Engineering, and the PhD degree in Physics from Politecnico di Torino, Italy, in 2004 and 2008, respectively. During 2008 he was a researcher fellow with the Electronics Department of the same institution, and since 2009 he is a Postdoctoral researcher at the Departament d'Enginyeria Electrònica, Universitat Autònoma de Barcelona, Spain. His research interests are mainly devoted to the physics-based simulation of transport in nano-devices, with special emphasis on the analysis and simulation of quantum correlations. Furthermore, he is also interested into the stability analysis of nonlinear circuits and systems, and into the noise analysis of nonlinear circuits.

Fabrizio Bonani was born in Torino, Italy, in 1967. He received the Laurea degree, *cum laude*, and the PhD degree in Electronic Engineering from Politecnico di Torino, Italy, in 1992 and 1996, respectively. Since 1995 he has been with the Electronics Department of the same institution, where he currently is an Associate Professor of Electronics. His research interests are mainly devoted to the physics-based simulation of semicondutor devices, with special emphasis on the noise analysis of field-effect and bipolar transistors, to the thermal analysis of power devices and circuits, and to the simulation and design of power semiconductor devices. He is also interested into the stability analysis of nonlinear circuits and systems, and into the noise analysis of nonlinear circuits.

From October 94 to June 95 he has been with the ULSI Technology Research Department of Bell Laboratories in Murray Hill (NJ) as a consultant, working on physics-based noise modelling of electron devices. From August to October 2008 he was Visiting Scientist at the Ferdinand-Braun-Institut für Höchstfrequenztechnik, Berlin, Germany, developing compact noise models for linear and nonlinear applications.

Prof. Bonani is Senior Member of IEEE, and the vice-chair of the MTT-14 Technical Committee on Low-Noise Techniques. He serves in the Modeling and Simulation committee of the International Electron Device Meeting for years 2010-2011.